

## Covalently Cross-Linked Colloidosomes

K. L. Thompson,<sup>†</sup> S. P. Armes,<sup>\*,†</sup> J. R. Howse,<sup>‡</sup> S. Ebbens,<sup>‡</sup> I. Ahmad,<sup>§</sup> J. H. Zaidi,<sup>§</sup>  
D. W. York,<sup>⊥</sup> and J. A. Burdis<sup>⊥</sup>

<sup>†</sup>Department of Chemistry, University of Sheffield, Brook Hill, Sheffield, South Yorkshire, S3 7HF, U.K.,

<sup>‡</sup>Department of Chemical & Biological Engineering, University of Sheffield, Mappin Street, Sheffield, S1 3JD, U.K.,

<sup>§</sup>Department of Chemistry, Faculty of Natural Sciences, Quaid-i-Azam University, Islamabad, 45320, Pakistan, and <sup>⊥</sup>Procter & Gamble, Newcastle Technical Centre, Whitley Road, Longbenton, Newcastle-upon-Tyne, NE12 9TS, U.K.

Received November 3, 2010

**ABSTRACT:** Model poly(glycerol monomethacrylate)-based macromonomers have been used to prepare sterically stabilized polystyrene latexes by either aqueous emulsion or alcoholic dispersion polymerization, affording mean latex diameters of approximately 107 or 1188 nm respectively as judged by dynamic light scattering. Such PGMA<sub>50</sub>–PS latexes have appropriate surface wettability to stabilize 25–250  $\mu$ m oil-in-water Pickering emulsions, depending on the latex concentration and oil type. Colloidosomes were formed by covalent cross-linking of the hydroxyl-functional stabilizer chains from *within* the oil droplets using a polymeric diisocyanate (tolylene 2,4-diisocyanate-terminated poly(propylene glycol) [PPG-TDI]. This oil-soluble cross-linker was confined within the oil droplets, allowing colloidosomes to be prepared at 50 vol % solids without any aggregation. The resulting microcapsules survive removal of the internal oil phase using excess alcohol, unlike the noncross-linked Pickering emulsion precursor. These observations confirm the robust nature of these covalently stabilized colloidosomes. A method for controlling the permeability of these colloidosomes by exploiting the solvent properties of binary oil mixtures has also been evaluated. Finally, microcapsule permeability has been explored via dye release experiments. Less permeable microcapsules can be obtained by deposition of polypyrrole onto the colloidosome exterior.

### Introduction

Colloidosomes are microcapsules whose shells are composed of colloidal particles that have been fused together to provide additional stability.<sup>1</sup> In recent years colloidosomes have received considerable attention due to their potential importance in the area of microencapsulation. Microencapsulation allows the controlled release of active ingredients in industrial sectors such as medicine, home and personal care products, agrochemicals, and cosmetics, delivering actives such as drugs, pesticides, insecticides, and fragrances. Routes to colloidosomes are commonly based on the self-assembly of colloidal particles at the interface between two immiscible liquids, typically water and oil; such so-called Pickering emulsions have been recognized for over a century.<sup>2</sup> A wide range of particles such as silica sols<sup>3,4</sup> and polystyrene latexes<sup>5</sup> have been shown to be effective Pickering emulsifiers. Stimulus-responsive particulate emulsifiers have also been developed, with rapid demulsification being achieved in response to changes in solution pH<sup>6–10</sup> or temperature.<sup>11,12</sup> The preparation of colloidosomes involves reinforcement of the particles adsorbed at the interface of these Pickering emulsions in order to form more robust, and ideally less permeable, microcapsule shells.

Velev and co-workers reported the first colloidosome-type structures in 1996 where latex particles were adsorbed onto emulsion droplet templates.<sup>13–15</sup> This group described the formation of both hollow spherical “supraparticles”<sup>13</sup> where surfactant-sensitized latex particles were adsorbed at the water/n-octanol interface and also “ball-like aggregates”<sup>14</sup> where the latex particles penetrated the bulk of the oil droplets. The term “colloidosome”

was first introduced by Dinsmore et al.,<sup>16</sup> who prepared microcapsules by the self-assembly of micrometer-sized polystyrene or poly(methyl methacrylate) latex particles at the surface of either oil-in-water or water-in-oil emulsion droplets. Once the droplet surface was covered by particles the colloidosome shell was formed by thermal annealing, whereby the emulsion was heated to just above the  $T_g$  of the polystyrene latex particles ( $\sim 105^\circ\text{C}$ ) using a glycerol cosolvent. Laib and Routh used a low  $T_g$  poly(styrene-*co*-*n*-butyl acrylate) latex to prepare colloidosomes<sup>17</sup> that could be annealed under relatively mild conditions, typically between 35 and 65  $^\circ\text{C}$ . Another form of colloidosome stabilization utilized an aqueous gelator within the internal phase.<sup>18</sup> Here in situ gelation ensures structural integrity; both “hairy”<sup>19</sup> and “magnetic”<sup>20</sup> colloidosomes have been prepared by this route.

Very few papers describe colloidosome stabilization by covalent cross-linking. Poly(divinylbenzene-*alt*-maleic anhydride) microspheres assembled at the oil/water interface have been cross-linked from the aqueous continuous phase by addition of polyamines.<sup>21</sup> Skaff and co-workers<sup>22</sup> assembled norbornene-functionalized CdSe/ZnS quantum dots at the water/toluene interface and then conducted ring-opening metathesis polymerization (ROMP) using a water-soluble Ru-based Grubbs catalyst to lock in the quantum dot superstructure. More recently, Shah et al.<sup>23</sup> prepared water-in-oil emulsions using primary amine-functionalized poly(*N*-isopropylacrylamide) microgels, followed by cross-linking within the aqueous droplets using glutaraldehyde to produce novel thermo-responsive microcapsules.

We recently reported the formation of colloidosomes via the chemical cross-linking of sterically stabilized latex particles at the oil–water interface.<sup>24</sup> Well-defined poly(glycerol monomethacrylate) macromonomers<sup>25</sup> allowed the synthesis

\*Corresponding author.

Table 1. Summary of the three sterically-stabilized latexes prepared using the PGMA<sub>50</sub> macromonomer

entry no.	SEM diameter/nm	DCP diameter/nm	DLS diameter (PDI)/nm	stabilizer content/%	$\Gamma/\text{mg m}^{-2}$
1	80	112 ± 14	107 (0.04)	9.8	1.5
2	837	851 ± 71	1188 (0.06)	0.9	1.3
3 <sup>a</sup>	813	893 ± 59	1015 (0.08)	1.1	1.6

<sup>a</sup> Contains 1 wt % fluorescein-*o*-methacrylate comonomer (based on styrene).

of near-monodisperse sterically stabilized latexes. Colloidosomes were formed by cross-linking the hydroxy-functional stabilizer chains using an *oil-soluble polymeric diisocyanate* from within the Pickering emulsion droplets.<sup>24</sup> In the current work, we extend our previous studies to explore these new covalently stabilized colloidosomes in more detail. In particular, we compare the relative merits of covalent cross-linking and thermal annealing for colloidosome formation. Laser diffraction is used to examine whether intercolloidosome fusion occurs during either cross-linking or thermal annealing at 50 vol % solids. We also examine the effect of latex concentration on the mean diameter of *n*-dodecane droplets and use these data to determine packing efficiencies for both small and large latexes adsorbed on the oil droplet surface. Dye release studies are conducted to assess the encapsulation efficiency of colloidosomes derived from such Pickering emulsions.

### Experimental Details

**Materials.** Glycerol monomethacrylate (GMA) was kindly donated by Cognis U.K. Ltd. (Hythe, U.K.) and used without further purification. 4-Vinylbenzyl chloride (4-VBC; 90%), Cu(I)Cl (99.995%), 2,2'-bipyridine (bpy, 99%), *n*-dodecane, sunflower oil, fluorescein, and tolylene 2,4-diisocyanate-terminated poly(propylene glycol) [PPG-TDI] were all purchased from Aldrich and were used as received. Styrene and pyrrole (Aldrich) were passed through a column of basic alumina to remove inhibitor and then stored at −20 °C prior to use. 2,2'-Azobis(isobutyronitrile) (AIBN; BDH) and ammonium persulfate (APS, Aldrich) were used as received. Methanol and ethanol were purchased from Fisher and were used as received. Deionized water was used in all experiments. Silica gel 60 (0.0632–0.2 mm) was obtained from Merck (Darmstadt, Germany). NMR solvents (D<sub>2</sub>O, CD<sub>3</sub>OD, CDCl<sub>3</sub>, and pyridine-*d*<sub>5</sub>) were purchased from Fisher.

**Homopolymerization of GMA.** *N*-(Dimethylamino)ethyl-2-bromoisobutyrylamide initiator (0.30 g, 1.25 mmol, prepared as reported previously<sup>25</sup>), bpy (0.39 g, 2.5 mmol) and GMA (10.0 g, 62.4 mmol, target  $D_p = 50$ ) were weighed into a 25 mL round-bottomed flask and degassed. Methanol (12.0 mL) was degassed and transferred into the reaction solution under nitrogen. The Cu(I)Cl catalyst (0.120 g, 1.25 mmol) was added to the stirred solution which turned dark brown, indicating the onset of polymerization. After 24 h, the reaction solution was diluted with methanol and passed through a silica column to remove the spent Cu(II) catalyst. The product was then dried on a vacuum line overnight to afford a white powder (8.0 g; yield = 77%).

**Macromonomer Synthesis via Quaternization.** The PGMA<sub>50</sub> homopolymer (7.0 g, 0.85 mmol) was dissolved in methanol (20 mL). 4-VBC (0.43 g, 2.55 mmol; 4-VBC/tertiary amine molar ratio = 3:1) was added and the reaction solution stirred at room temperature for 48 h. Excess unreacted 4-VBC was removed by precipitation into cyclohexane and the precipitated polymer was dried under vacuum overnight to afford a white powder (6.0 g; yield = 84%).

**Aqueous Emulsion Polymerization.** PGMA<sub>50</sub> macromonomer (0.500 g) was weighed into a 100 mL round-bottomed flask and dissolved in water (50.0 g). This solution was purged with nitrogen for 30 min before being heated to 70 °C under a nitrogen blanket. The AIBN initiator (0.050 g) was dissolved in styrene (5.00 g) and purged with nitrogen before being injected into the reaction vessel. The solution turned milky-white within 1 h

and was stirred for 24 h. The latex was purified by three centrifugation/redispersion cycles, replacing each successive supernatant with pure water. The mean diameter of the resulting latex particles was assessed by scanning electron microscopy, disk centrifuge photosedimentometry, and dynamic light scattering (see Table 1).

**Alcoholic Dispersion Polymerization.** PGMA<sub>50</sub> macromonomer (0.500 g) was weighed into a 100 mL three-necked round-bottomed flask fitted with a condenser and nitrogen inlet and dissolved in a 9:1 methanol/water mixture (50.0 g). This solution was purged with nitrogen for 30 min before being heated to 70 °C under a nitrogen blanket. The AIBN initiator (0.050 g) was dissolved in styrene (5.00 g) and purged with nitrogen before being injected into the reaction vessel. The solution turned milky-white within 1 h and was stirred for 24 h. The latex was purified by three centrifugation/redispersion cycles replacing each successive supernatant with the 9:1 methanol/water mixture, followed by three redispersion cycles into pure water. The mean diameter of the resulting latex particles was assessed by scanning electron microscopy, disk centrifuge photosedimentometry and dynamic light scattering (see Table 1). The above protocol was repeated utilizing 0.050 g fluorescein-*o*-methacrylate (1 wt % based on styrene) to prepare a fluorescently labeled latex for fluorescence microscopy experiments, see Table 1 for particle size details. For clarity, each of the latexes used in this study will be denoted by their intensity average diameter.

**Colloidosome Preparation.** PPG-TDI (0.025 g) was weighed into a sample vial and then dissolved in 5.0 mL oil (e.g., *n*-dodecane, sunflower oil, or isononyl isononate). This solution was then homogenized with 5.0 mL of 0.4–10.0 wt % aqueous latex for 2 min using a IKA Ultra-Turrax T-18 homogenizer with a 10 mm dispersing tool operating at 12,000 rpm. The resulting stable milky-white emulsion was allowed to stand at 20 °C for 0–60 min to allow the cross-linking reaction to proceed.

**Cyclohexane Annealing of Colloidosomes.** Colloidosomes were prepared as described above, but using 5.0 mL of a 4:1 *n*-dodecane/cyclohexane mixture as the oil phase instead of pure *n*-dodecane. The resulting stable milky-white emulsion (average droplet diameter = 99 ± 80 μm) was split between five vials, with four of these emulsions being heated to 50 °C in an oven for 15, 30, 45, and 60 min, respectively.

**Encapsulation and Release of Fluorescein from Colloidosomes.** Fluorescein (1.0 mg) was weighed into a glass sample vial, along with PPG-TDI (0.025 g). This was then dissolved in the sunflower oil (5.0 mL) before homogenization with a 5.0 wt % of a 1188 nm PGMA<sub>50</sub>–PS aqueous latex for 2 min. The resulting emulsion was allowed to stand at 20 °C for 30 min to allow the cross-linking reaction to proceed. Release studies were conducted using a PC-controlled Perkin-Elmer Lambda 25 uv/visible absorption spectrophotometer operating in time drive mode. A known mass (0.020–0.024 g) of filtered colloidosomes (or polypyrrole-coated colloidosomes, see below) was placed on top of an aqueous solution (3.0 mL, pH 9) in a disposable UV-grade cuvette equipped with a miniature magnetic stirrer bar. The absorbance at 490 nm due to the released dye was monitored as a function of time. Since the colloidosomes are less dense than water they remain buoyant and out of range of the transmitted beam. As a control experiment, pure oil containing the same concentration of dissolved dye was used instead of colloidosomes.

**Polypyrrole Deposition onto Colloidosomes.** Fluorescein-encapsulated cross-linked colloidosomes (2.0 mL of a 50 vol % dispersion of  $89 \pm 24 \mu\text{m}$  colloidosome microcapsules) were transferred into a sample vial. Ammonium persulfate (0.019 g; 0.083 mmol) and pyrrole monomer (0.005 mL; 0.075 mmol) were added to these colloidosome microcapsules, followed by mixing for 16 h at 20 °C using a roller mixer. This protocol produced polypyrrole-coated colloidosomes with a conducting polymer mass loading of 0.66 wt % (approximate target polypyrrole thickness 60 nm). Another 2.0 mL aliquot was coated with 1.32 wt % polypyrrole (using 0.038 g APS and 0.01 mL pyrrole). The average thickness,  $x$ , of the deposited polypyrrole overlayer on the colloidosomes can be calculated using eq 1<sup>26</sup>

$$x = R \left[ \left( \frac{M_{\text{ppy}} \rho_{\text{oil}}}{M_{\text{oil}} \rho_{\text{ppy}}} + 1 \right)^{1/3} - 1 \right] \quad (1)$$

where  $R$  = the radius of the original uncoated colloidosomes (as judged by Malvern Mastersizer),  $M_{\text{ppy}}$  and  $\rho_{\text{ppy}}$  are the mass fraction and density of the polypyrrole component, and  $M_{\text{oil}}$  and  $\rho_{\text{oil}}$  are the mass fraction and density of the oil droplet component. It was assumed that the adsorbed PS latex has minimal effect on the droplet radius, density, or mass fraction and so this component was not included in the calculation.

**Polymer Characterization.** <sup>1</sup>H NMR Spectroscopy. All <sup>1</sup>H NMR spectra were recorded in either CDCl<sub>3</sub>, D<sub>2</sub>O, CD<sub>3</sub>OD, or pyridine-*d*<sub>5</sub> using a 400 MHz Bruker Avance-400 spectrometer.

**DMF GPC.** The molecular weight and polydispersity of the PGMA homopolymer precursor were determined by DMF GPC at 70 °C. The GPC setup comprised three Polymer Laboratories PL gel 10  $\mu\text{m}$  "Mixed B" columns in series with a Viscotek TriSEC model 302 refractive detector. The flow rate was 1.0 mL min<sup>-1</sup> and the mobile phase contained 10 mmol LiBr. Ten near-monodisperse PMMA standards ( $M_p = 2000\text{--}300\,000 \text{ g mol}^{-1}$ ) were used for calibration purposes and data were analyzed using Viscotek TriSEC 3.0 software.

**Dynamic Light Scattering (DLS).** Intensity-average hydrodynamic diameters of the three latexes were obtained by DLS using a Malvern Zetasizer NanoZS instrument. Aqueous dispersions of 0.01 wt % latex were analyzed using disposable cuvettes, and the results were averaged over three consecutive runs. The deionized water used to dilute each latex was ultra-filtered through a 0.20  $\mu\text{m}$  membrane so as to remove dust.

**Colloidosome Characterization.** *Conductivity Measurements.* The conductivities of the emulsions immediately after preparation were measured using a digital conductivity meter (Hanna model Primo 5). A high conductivity (typically  $> 10 \mu\text{S cm}^{-1}$ ) indicated that all emulsions in this work were water-continuous. These results were confirmed using the so-called "drop test": one drop of the emulsion was added to both pure water and oil, and its ease of dispersion was assessed by visual inspection. Relatively rapid dispersion into water was observed in all cases, which confirmed that the continuous phase of the emulsion was water.

**Laser Diffraction.** A Malvern Mastersizer 2000 instrument equipped with a small volume Hydro 2000SM sample dispersion unit (ca. 50 mL), a HeNe laser operating at 633 nm, and a solid-state blue laser operating at 466 nm was used to size the emulsions. The stirring rate was adjusted to 1,000 rpm in order to avoid creaming of the emulsion during analysis. The mean droplet diameter was taken to be the volume mean diameter ( $D_{4/3}$ ), which is mathematically expressed as  $D_{4/3} = \sum D_i^4 N_i / \sum D_i^3 N_i$ . The standard deviation for each diameter provides an indication of the size distribution. After each measurement, the cell was rinsed once with ethanol, followed by three times with doubly distilled water, the glass walls of the cell were carefully wiped with lens cleaning tissue to avoid cross-contamination and the laser was aligned centrally on the detector prior to measurements.

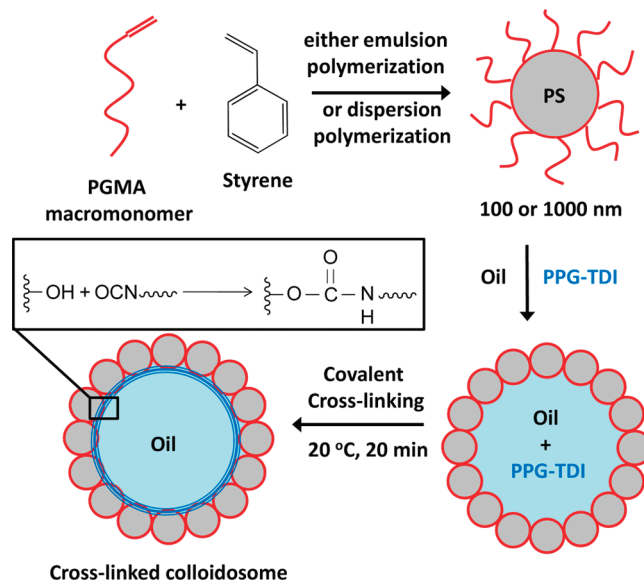


**Figure 1.** Covalently cross-linked colloidosomes prepared by self-assembly of PGMA<sub>50</sub>–PS latex particles around oil droplets in the presence of the oil-soluble PPG-TDI cross-linker.

**Optical Microscopy.** Optical microscopy images were recorded with a James Swift MP3502 microscope, (Prior Scientific Instruments Ltd.) fitted with a digital camera (Nikon Coolpix 4500).

**Fluorescent Microscopy.** Parallel fluorescence and brightfield microscopy was carried out using a Nikon Eclipse LV100 microscope. The fluorescence excitation and emission wavelengths were controlled by a B-2A filter block (Nikon). Fluorescent images were captured using a high sensitivity EMCCD Andor iXon+ 897 camera (512 × 512 pixels). Brightfield (diascopic) images were captured using a Luminera 2.1 CCD camera.

**Scanning Electron Microscopy (SEM).** SEM studies were performed using a FEI Sirion field emission scanning electron microscope using a beam current of 244  $\mu\text{A}$  and a typical operating voltage of 20 kV. Colloidosome samples were washed repeatedly with ethanol to remove any traces of oil. Samples were dried onto aluminum stubs and sputter-coated with a thin layer of gold prior to examination so as to prevent sample charging.

**Packing Efficiency Calculation.** According to the recent work of Balmer et al.,<sup>27</sup> the following equation was used to estimate a packing efficiency ( $P$ ) for 107 nm PGMA<sub>50</sub>–PS particles adsorbed onto *n*-dodecane droplets:

$$N = \frac{4P(r_d + r_l)^2}{r_l^2} \quad (2)$$

where  $N$  = number of latex particles per oil droplet,  $P$  = latex packing efficiency,  $r_d$  = mean radius of the oil droplet (as determined by laser diffraction), and  $r_l$  = mean radius of the latex particles (as determined by DLS).  $P$  was calculated for lower latex concentrations (0.35–1.2 wt %) where it was determined (by visual inspection of the creamed emulsion) that essentially all latex particles in solution had adsorbed onto the oil droplets (this was confirmed by gravimetric analysis of the aqueous phase formed below the creamed emulsion).

## Results and Discussion

The synthetic route for the preparation of covalently cross-linked colloidosomes starting from well-defined poly(glycerol monomethacrylate) macromonomers is outlined in Figure 1. The first step is to prepare PGMA<sub>50</sub>–PS latexes via either aqueous emulsion or alcoholic dispersion polymerization.<sup>25</sup>



Transmission and scanning electron micrographs of two such latexes are shown in Figure 2 and particle characterization data for the three latexes used in this work appears in Table 1. These latexes were then homogenized with various oils to obtain oil-in-water Pickering emulsions.

Having determined that these emulsions were always of the oil-in-water type (via conductivity measurements and the drop-test) a suitable cross-linker was selected. An oil-soluble cross-linker was considered desirable since this avoids the need to remove any excess cross-linker and should also confine the cross-linking reaction to within the oil droplets. Thus, cross-linking only occurs within individual colloidosomes rather than between them, allowing their production at high solids (50 vol %). The cross-linker chosen was tolylene 2,4-diisocyanate-terminated poly(propylene glycol) [PPG-TDI], which readily reacts with the hydroxy groups from the PGMA stabilizer to form robust urethane bonds with no small molecule byproduct. This commercially available polymeric cross-linker is significantly less toxic than small molecule diisocyanates because it is nonvolatile. Moreover, its insolubility in water prevents partitioning between the oil droplets and the aqueous continuous phase. PPG-TDI was dissolved in the oil phase prior to emulsification; after homogenization the Pickering emulsion was simply allowed to stand without stirring at room temperature for 20–30 min to allow cross-linking to occur.<sup>24</sup> In principle, cross-linking can occur between OH groups on the same latex particle as well as between neighboring latex particles. However, calculation of the effective isocyanate/OH molar ratio used during the preparation of these cross-linked colloidosomes is somewhat problematic, since this depends on the contact angle made between the latex particles and the oil phase (and this

parameter is not known). If we assume that this oil-latex contact angle is 90°, which is almost certainly an overestimate, we calculate an isocyanate/OH molar ratio of approximately 1:1 for the 107 nm PGMA<sub>50</sub>–PS latex when employed at a concentration of 1.0 wt % (assuming that all the PGMA<sub>50</sub> macromonomer chains are located at the latex surface and all the latex is adsorbed onto the oil droplets). Thus, there is sufficient polymeric cross-linker to react with every single hydroxy group located at the oil droplet surface. This suggests that significant wastage of the PPG-TDI cross-linker can occur via *intraparticle* cross-linking while still allowing efficient *interparticle* cross-linking to be achieved.

Table 2 shows the volume-average droplet diameter,  $D_{4/3}$ , obtained for cross-linked colloidosomes prepared using the three latexes with either *n*-dodecane, sunflower oil or isononyl isononanoate as the oil phase. *n*-Dodecane was chosen as a model oil for further studies. It was found that increasing the latex concentration in the aqueous phase reduces the mean droplet diameter, as expected.<sup>28</sup> Also, a significantly higher concentration of the larger latexes (entries 2 and 3, Table 1) is required compared to the smaller latex (entry 1, Table 1) to compensate for the much lower specific surface areas of the former emulsifiers. In most cases high latex adsorption efficiency is obtained during colloidosome construction, often with more than 99% of the latex becoming adsorbed at the oil–water interface and negligible excess latex remaining in aqueous solution.

Figure 3 shows the relationship between the latex concentration and mean droplet diameter of colloidosomes prepared with the 107 nm PGMA<sub>50</sub>–PS latex. Increasing the latex concentration decreases the mean droplet diameter, until a plateau at 25  $\mu$ m is reached. Higher latex concentrations do not lead to any further reduction in droplet size but merely to excess latex particles in solution. This observation is consistent with those reported previously.<sup>28,29</sup> In those cases where no excess latex could be detected in solution, a packing efficiency ( $P$ ) for the particles adsorbed onto the *n*-dodecane droplets was calculated using an equation previously reported by Balmer et al. for large latex particles coated with small silica particles.<sup>27</sup> In the case of *n*-dodecane droplets stabilized by the 107 nm PGMA<sub>50</sub>–PS latex particles, a packing efficiency of 0.85 is calculated. Hexagonal close packing of spheres on a planar surface leads to a maximum  $P$  value of 0.91,<sup>27</sup> but the curvature of the oil droplet surface will inevitably lead to packing defects that lower the theoretical packing efficiency. Balmer et al. examined the packing efficiency of a relatively polydisperse 20 nm silica sol onto a monodisperse poly(2-vinylpyridine) (P2VP) latex core.<sup>27</sup> They found an experimental packing efficiency of  $0.69 \pm 0.04$ , which was somewhat lower than the calculated theoretical maximum packing efficiency of  $0.86 \pm 0.04$ . This maximum  $P$  value was calculated by

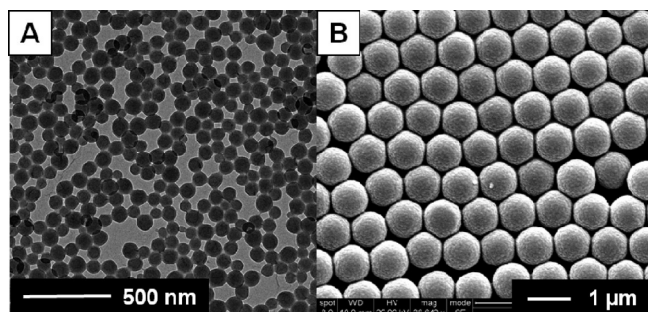


**Figure 2.** Transmission electron microscopy image of A) 107 nm PGMA<sub>50</sub>–PS latex particles prepared by aqueous emulsion polymerization (entry 1, Table 1) and scanning electron microscopy image of B) 1188 nm PGMA<sub>50</sub>–PS latex particles prepared by alcoholic dispersion polymerization (entry 2, Table 1).

**Table 2.** Summary of the Mean Droplet Diameter and Latex Incorporation Efficiency for Various Oil-in-Water Colloidosomes Prepared Using Three PGMA<sub>50</sub>–PS Latexes and PPG-TDI Cross-Linker with *n*-Dodecane, Sunflower Oil, and Isononyl Isononanoate as the Oil Phase<sup>a</sup>

latex	latex diameter (DLS)/nm	oil	latex concentration/wt %	droplet diameter/ $\mu$ m	latex adsorption efficiency <sup>b</sup> /%
1	107	<i>n</i> -dodecane	0.35	112 $\pm$ 47	> 99
			0.66	59 $\pm$ 28	> 99
			0.8	49 $\pm$ 23	> 99
			1.2	33 $\pm$ 17	> 99
			2.00	26 $\pm$ 13	89
			3.46	25 $\pm$ 12	51
			5.00	25 $\pm$ 14	36
			5.00	25 $\pm$ 14	36
2	1188	<i>n</i> -dodecane	1.90	225 $\pm$ 115	> 99
			2.70	160 $\pm$ 94	> 99
			4.80	91 $\pm$ 35	> 99
			9.40	60 $\pm$ 28	80
		sunflower oil	5.00	65 $\pm$ 25	95
		isononyl isononanoate	5.00	83 $\pm$ 32	90
3	1015	<i>n</i> -dodecane	5.00	92 $\pm$ 48	80

<sup>a</sup> 5.0 mL of aqueous latex was homogenized at 12 000 rpm for 2 min with 5.0 mL of oil containing 0.025 g of PPG-TDI cross-linker. <sup>b</sup> As judged by gravimetric analysis of the creamed aqueous phase.

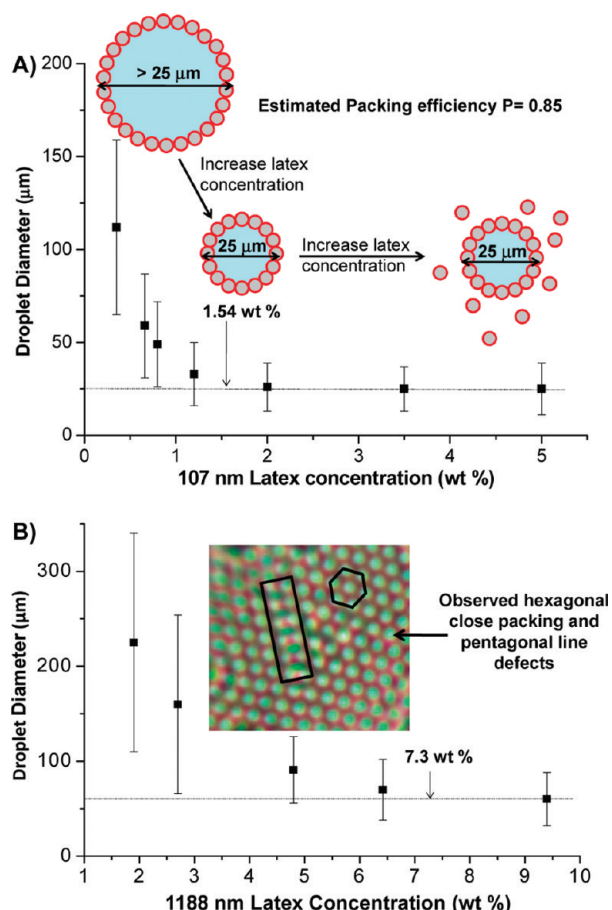


**Figure 3.** Relationship between latex concentration and mean droplet diameter for colloidosomes prepared with (A) 107 nm PGMA<sub>50</sub>-PS particles using *n*-dodecane as the oil phase. The minimum droplet diameter is 25  $\mu\text{m}$ , with further increase in latex concentration leading to excess particles in solution and (B) 1188 nm PGMA<sub>50</sub>-PS particles using *n*-dodecane as the oil phase. The minimum droplet diameter is 60  $\mu\text{m}$ . An estimated packing efficiency of 0.85 was calculated in both cases.

taking into account the curvature of the small silica sol packing onto the core particle. In the current work, adsorbing a 107 nm latex onto 25  $\mu\text{m}$  oil cores leads to significantly less curvature of the droplet surface due to the larger difference between the latex and droplet diameters. Therefore, the approximation made in deriving eq 2 is less likely to incur any significant error. A packing efficiency of 0.85 is a reasonable value for this colloidosome system, since it lies between that observed experimentally for the silica/P2VP nanocomposite system and perfect hexagonal packing on a planar surface (0.69 and 0.91, respectively). Using  $P = 0.85$  it was calculated that the minimum concentration of 107 nm latex required for monolayer coverage of a 25  $\mu\text{m}$  droplet should be 1.54 wt %, which is consistent with the experimental data shown in Figure 3A. Therefore, under these particular emulsification conditions there is no significant advantage in using latex concentrations above this upper limit of 1.54 wt %, since the droplet diameter will remain constant at 25  $\mu\text{m}$  and any excess latex simply resides in the aqueous phase. A value of  $P$  for the larger 1188 nm latex packing around *n*-dodecane droplets was also calculated (again for the cases where no excess latex could be detected in solution, see Table 2 and Figure 3B). The same packing efficiency of 0.85 was obtained in this case, with a limiting droplet diameter of 60  $\mu\text{m}$  being achievable at a latex concentration of 7.3 wt % or above (see Figure 3B). This suggests that efficient packing of these monodisperse PGMA<sub>50</sub>-PS latex spheres is achievable irrespective of the latex size. Thus, there

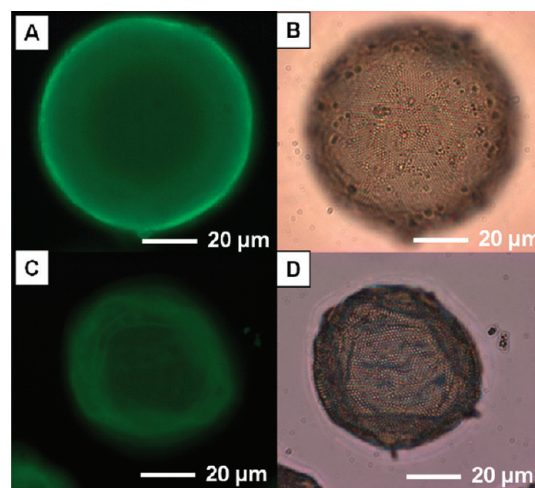


**Figure 4.** (A) Fluorescence microscopy image of a PPG-TDI cross-linked colloidosome prepared with 1015 nm fluorescently labeled PGMA<sub>50</sub>-PS latex and *n*-dodecane (B) bright field image of the same colloidosome (note that the individual latex particles on the colloidosome surface can be resolved). (C) Fluorescent microscopy image of the collapsed colloidosome obtained after washing with excess ethanol (D) bright field image of the same ethanol washed colloidosome (again the individual latex particles can be seen).

appears to be an optimum latex concentration for a given latex diameter and oil type that enables the minimum droplet diameter to be obtained with essentially all the latex particles being adsorbed onto the oil droplets with comparable packing efficiencies.

The inset in Figure 3B shows a high magnification optical microscopy image of a typical individual colloidosome microcapsule prepared with 1015 nm fluorescently labeled latex particles in which hexagonal close-packing of the latex spheres is clearly observed, along with the boundary scar defects reported by Bausch and co-workers that are characteristic of the packing of small spheres around a larger sphere.<sup>30</sup>

Successful cross-linking was assessed by an alcohol challenge, whereby a small aliquot of colloidosome was diluted with excess ethanol (which is a common solvent for both the water and oil phases)<sup>31</sup> and observed by optical and fluorescence microscopy (see Figure 4).

When the noncross-linked Pickering emulsion is subjected to such a challenge, no microcapsules are observed by optical microscopy and only latex debris is visible by SEM (Figure 5A). In contrast, when covalently cross-linked colloidosomes are challenged with ethanol, intact microcapsules are observed by both optical and scanning electron microscopy. Figure 5B and 5C shows SEM images of colloidosomes prepared with either 107 or 1188 nm PGMA<sub>50</sub>-PS latex (see entries 1 and 2 in Table 1). Such capsules also collapse during ethanol evaporation (i.e., prior to UHV conditions). A lower magnification image shows a large population of cross-linked colloidosomes observed for a typical sample, showing that this is an efficient route to produce colloidosomes.

This alcohol challenge has also been utilized to establish that a time scale of around 20 min is required for the formation of intact colloidosomes using PPG-TDI cross-linker at room temperature.<sup>24</sup> This cross-linking reaction can also be conveniently monitored by <sup>1</sup>H NMR spectroscopy, at least in the case of the 107 nm latex<sup>24</sup> (see Figure S1 in the Supporting Information). In the present work, NMR analysis of dried cross-linked colloidosomes prepared with the 1188 nm latex was also attempted. In this case, the PPG-TDI peaks were barely detectable due to the larger latex diameter (and correspondingly much lower PGMA content). FT-IR spectra were also recorded for these dried cross-linked colloidosomes (see Figure S2 in the Supporting Information).



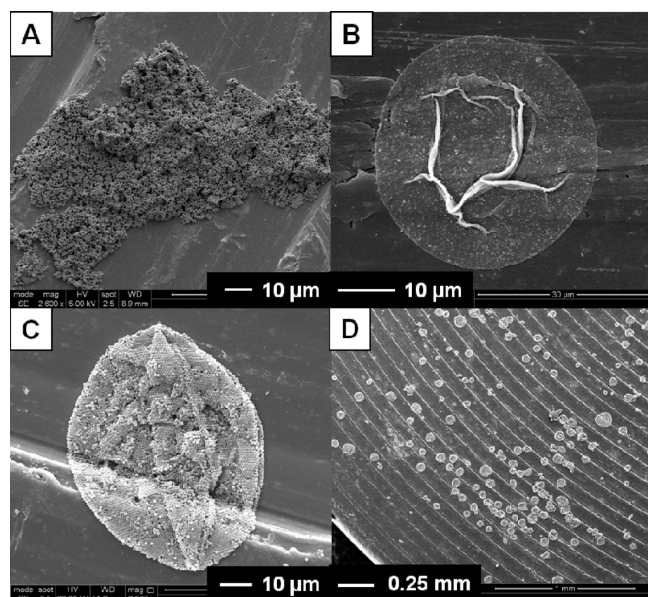


**Figure 5.** Scanning electron microscopy images obtained after ethanol challenges of (A) latex debris obtained with a noncross-linked Pickering emulsion prepared with 5.0% 1188 nm PGMA<sub>50</sub>-PS particles, (B) cross-linked colloidosomes prepared with 1.0% 107 nm PGMA<sub>50</sub>-PS particles, (C) cross-linked colloidosomes prepared with 5.0% 1188 nm PGMA<sub>50</sub>-PS particles and (D) lower magnification image of sample C showing multiple colloidosomes. The oil phase was *n*-dodecane in each case.

Unfortunately it was not possible to confirm the presence of the new urethane bonds, since this band overlaps with the ester carbonyl band from the GMA units. However, a prominent band at 1097 cm<sup>-1</sup> was observed in the spectra obtained for both the cross-linker and the washed/dried colloidosomes. This feature is assigned to the C–O stretch due to the PPG repeat units of the cross-linker. This again supports our findings that the PPG-TDI reacts with the GMA units on the latex surface and becomes covalently bound.

Laser diffraction studies confirmed that the cross-linking is indeed confined to the droplet phase, as expected. Figure 6 shows representative droplet size distributions recorded for freshly prepared covalently cross-linked colloidosomes, on standing for 3 and 330 h after homogenization. Immediately after homogenization cross-linking was not yet complete, as judged by the alcohol challenge and optical microscopy studies. Thus, the initial droplet size distribution is essentially that of the original Pickering emulsion. Three hours after homogenization, intact colloidosomes are observed by optical microscopy, but minimal change is observed in the volume-average droplet diameter. A similar size distribution was obtained 330 h after the initial homogenization. This indicates that the PPG-TDI cross-linker is indeed confined to the oil phase and minimal intercolloidosome cross-linking occurs even at 50 vol % solids. Very recently, we have also obtained similar results for covalently cross-linked colloidosomes prepared using a polyamine-functionalized latex combined with three different polymeric cross-linkers.<sup>32</sup> This is a potentially important advance compared to previous cross-linking protocols.<sup>21</sup> Given the known high reactivity of diisocyanate groups toward water, a water-soluble equivalent of the oil-soluble PPG-TDI cross-linker is simply not feasible: such cross-linking chemistry must necessarily be restricted to the oil droplet phase.

Although robust colloidosomes can be obtained by PPG-TDI cross-linking alone, the resulting microcapsules are highly permeable due to their many interstitial pores between adjacent latex particles. Previous workers have shown that thermal annealing can reduce and perhaps close these interstices.<sup>16,17,33</sup> In principle,

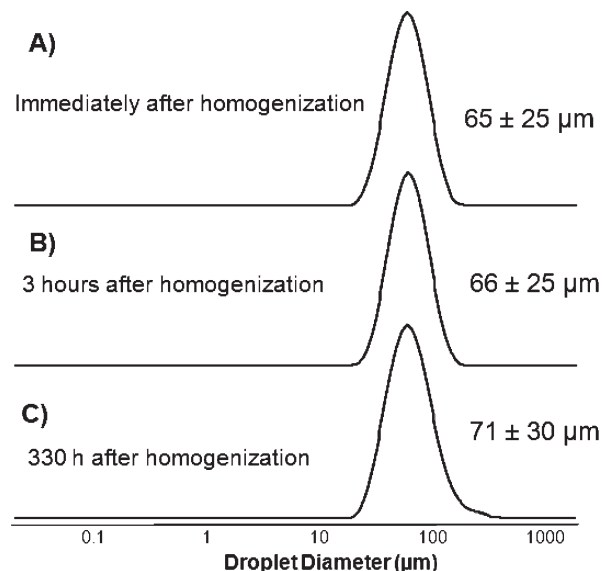


**Figure 6.** Laser diffraction particle size distribution curves obtained using a Malvern Mastersizer for cross-linked colloidosomes prepared with 1188 nm PGMA<sub>50</sub>-PS latex particles (5.0 wt %) and sunflower oil (A) immediately after homogenization (when cross-linking is incomplete as judged by an ethanol challenge combined with optical microscopy), (B) 3 h after homogenization when cross-linking is now complete and (C) 330 h (2 weeks) after homogenization. Little difference in these droplet size distributions is observed, confirming that minimal intercolloidosome fusion occurs during cross-linking since the cross-linker is confined to the oil phase.

this simply involves heating the latex particles to above their glass transition temperature, which for polystyrene is approximately 105 °C. However, annealing at such a temperature could have implications for the encapsulation of temperature-sensitive actives, and cannot be achieved for oil-in-water Pickering emulsions without the addition of high bp water-miscible cosolvents such as glycerol. In our previous work,<sup>24</sup> 20% cyclohexane was incorporated into the oil phase prior to emulsification at room temperature. On heating the cross-linked colloidosomes to 50 °C for 1 h, the cyclohexane cosolvent (the UCST for polystyrene in cyclohexane is 35 °C)<sup>34</sup> plasticized the latex particles and substantial annealing was observed well below the *T<sub>g</sub>* of the latex core. Similar observations have been recently made by Biggs and co-workers.<sup>35</sup> In the present work, we extend our preliminary studies by comparing the effect of cyclohexane annealing in both the presence and absence of the PPG-TDI cross-linker at 50 vol % solids and also explore the extent of intercolloidosome fusion that occurs under these conditions. In these experiments we focused on the 1188 nm latex, because colloidosome interstices formed by these larger particles are far easier to observe by SEM. Figure 7 shows SEM images of both cross-linked and noncross-linked samples prepared with the 1188 nm latex, before (A and B) and after (C and D) cyclohexane annealing at 50 °C for 60 min. Before heating, Figure 7A shows the latex debris that is always observed in the absence of cross-linking while Figure 7B shows an example of the collapsed colloidosome structure that is typically observed in the presence of cross-linker. After heating to 50 °C for 1 h both samples exhibit significant evidence for interstitial annealing, with microcapsules also being formed in the absence of any PPG-TDI cross-linker. However, it is emphasized that the yield of intact microcapsules prepared without any cross-linker is relatively low and many fractured and broken particles are observed by SEM under these conditions (see Figure S3 in the Supporting Information). In contrast, all the cross-linked colloidosomes that were visible on the SEM stub remained intact. Although partial collapse is still observed under the UHV

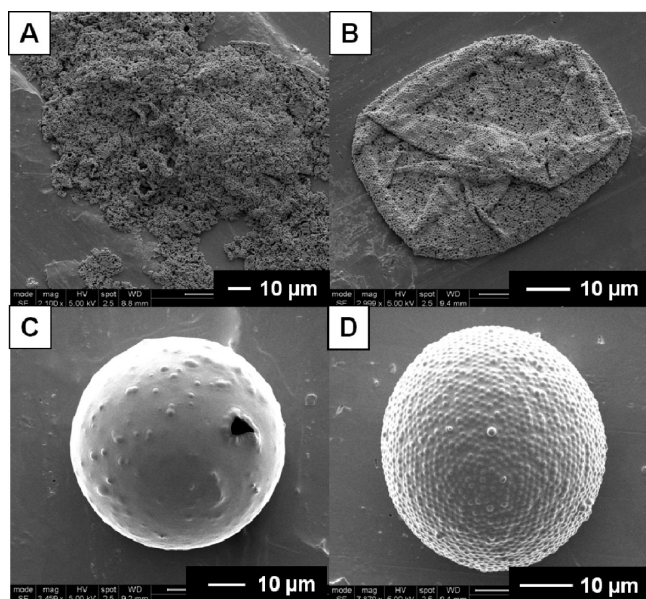


**Figure 7.** Scanning electron microscopy images of samples prepared using 5.0% 1188 nm PGMA<sub>50</sub>-PS latex particles and a 4:1 *n*-dodecane/cyclohexane oil mixture. (A) Only latex debris is observed in the absence of cross-linker at 20 °C. (B) A collapsed colloidosome is obtained in the presence of the PPG-TDI cross-linker at 20 °C. (C) A solvent-annealed colloidosome prepared in the absence of cross-linker after heating to 50 °C for 1 h. (D) A solvent-annealed and cross-linked colloidosome prepared in the presence of PPG-TDI cross-linker after heating to 50 °C for 1 h. Note that covalent cross-linking of the latex particles appears to hinder the extent of annealing (compare the surface texture of C with D).

conditions required for these SEM studies, no rupture or breakage occurs compared to the noncross-linked capsules (see Figure S4 in the Supporting Information). However, Figure 7 also suggests that the extent of annealing achieved after 1 h appears to be somewhat reduced in the presence of cross-linker (since the microcapsule surface is not as smooth as that observed in the absence of cross-linker). This difference is attributed to the PPG cross-links between latex particles hindering latex coalescence.

It is also noteworthy that, unlike cross-linking alone, cyclohexane annealing at 50 vol % results in a substantial amount of intercolloidosome fusion, as illustrated in Figure 8. The droplet size distribution shifts to higher diameters for longer annealing times, which indicates partial agglomeration of the colloidosomes under these conditions. Significant dilution would be required to minimize this intercolloidosome fusion and hence ensure discrete microcapsules, which is not likely to be commercially attractive.

The encapsulation and release properties of these cross-linked colloidosomes were also investigated for a model dye. The dye was required to be initially oil-soluble to ensure effective encapsulation but be subsequently capable of triggered release on changing the external aqueous solution pH. Fluorescein ( $pK_a \sim 6.3$ ) was selected as an appropriate acid dye, since it is oil-soluble in its protonated form at low pH but becomes water-soluble at higher pH.<sup>36</sup> Sunflower oil was selected as the droplet phase in these release experiments since it dissolved the dye more easily than *n*-dodecane. It is perhaps worth emphasizing here that the cross-linking reaction between the PGMA and PPG-TDI appears to have little or no pH dependence, since it was equally successful at pH 3, 7, and 10. This is understandable, since only those PGMA chains on the inside of the colloidosomes (i.e., wetted by the oil phase) are available for reaction with the PPG-TDI. Therefore, oil-in-water colloidosomes were prepared at pH 3 with fluorescein encapsulated within the oil cores and dye release was subsequently triggered when desired by increasing the pH of the aqueous continuous phase above the  $pK_a$  of the dye

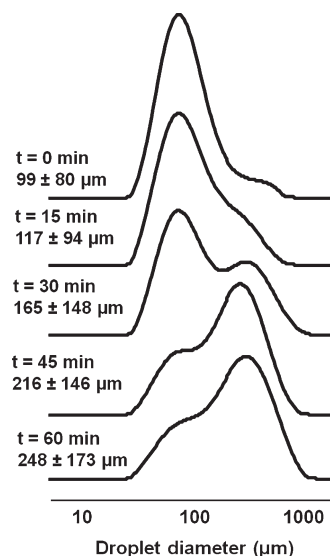


**Figure 8.** Laser diffraction particle size distribution curves obtained using a Malvern Mastersizer for cross-linked colloidosomes prepared with 1188 nm PGMA<sub>50</sub>-PS latex and 4:1 *n*-dodecane/cyclohexane oil phase after annealing at 50 °C for up to 1 h. The droplet size distribution shifts to higher diameters upon increasing the annealing time, demonstrating that neighboring capsules become fused together when annealing occurs at 50 vol %.

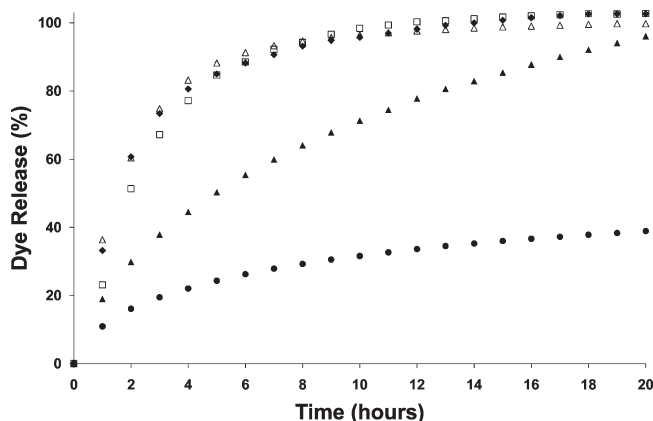


**Figure 9.** Release curves obtained at pH 9 for fluorescein dye diffusing from: sunflower oil control (closed diamonds), uncoated cross-linked colloidosomes prepared with 1188 nm PGMA<sub>50</sub>-PS particles (open squares), cyclohexane annealed colloidosomes (4:1 *n*-dodecane/cyclohexane oil phase, open triangles), cross-linked colloidosomes after coating with 0.66 wt % polypyrrole (closed triangles) and cross-linked colloidosomes after coating with 1.32 wt % polypyrrole (closed circles).

(see Figure S5 in the Supporting Information for visible absorption spectra and calibration plot of the dye at pH 9). To allow the rate of dye diffusion into the aqueous phase to be assessed when there was no microcapsule barrier, a control experiment was conducted whereby the release of fluorescein dye from sunflower oil alone was measured. Unfortunately, the solely cross-linked colloidosomes proved to be highly permeable, with little difference in the rate of dye release being observed between the control experiment and our cross-linked colloidosomes (see Figure 9).

Given that these particles contain a large number of interstitial holes (and defects) between adjacent latex particles, such permeability toward a small molecule dye is perhaps not surprising. Cyclohexane annealing, although appearing to close these interstitial holes as judged by SEM, did not significantly retard the rate of dye release compared to nonannealed cross-linked colloidosomes or



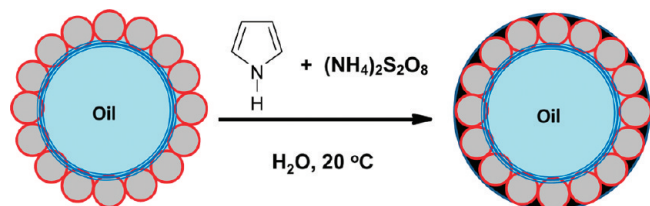


**Figure 10.** Schematic representation of the deposition of an ultrathin layer of polypyrrole (depicted as a black coating) onto covalently cross-linked colloidosomes from aqueous solution at 20 °C using ammonium persulfate oxidant at pH 2 (using HCl to adjust the solution pH).

the control experiment involving just sunflower oil, see Figure 9. We attribute this to the difficulty in ensuring that every single interstitial hole is closed in each colloidosome. Indeed, similar results were reported by Yow and Routh,<sup>33</sup> who investigated the release of fluorescein in its sodium salt form from the aqueous cores of colloidosomes annealed for 5–60 min at 49 °C. These workers found that, although longer latex annealing times did lead to slower release rates, dye retention remained surprisingly poor. All encapsulated dye was released within 24 h, despite SEM images that suggested smooth latex shells were obtained with no evidence for any interstitial defects. Such encapsulation times are obviously far too short for most commercial applications. We encountered similar difficulties in our release experiments with these covalently cross-linked colloidosomes, with or without cyclohexane annealing.

In order to address this problem, we deposited an thin layer of polypyrrole onto the cross-linked colloidosomes using a well-known aqueous deposition protocol previously developed by our group for micrometer-sized sterically stabilized polystyrene latexes.<sup>26</sup> Polypyrrole is a black insoluble electrically conducting polymer that can be readily synthesized in water at room temperature.<sup>37</sup> Since significant agglomeration of the colloidosomes occurred during cyclohexane annealing (see Figure 8) and this annealing appeared to offer no additional benefit in terms of retarding the rate of dye release, nonannealed cross-linked colloidosomes were used for the polypyrrole coating experiments. The polymerization of pyrrole requires an acidic solution (pH < 2), but since the fluorescein dye remains water-insoluble at low pH, it is not affected by the polypyrrole deposition conditions and is retained within the oil droplets.

Figure 10 shows a schematic representation of the polypyrrole deposition onto the outside of a cross-linked colloidosome. The coating formulation is such that essentially all of the polypyrrole is deposited onto the surface of the colloidosomes, with no little or no polypyrrole precipitating in the bulk aqueous solution.<sup>26</sup>

Figure 11 shows the SEM images of the colloidosomes prepared with the 1188 nm latex both before and after conducting polymer deposition. Polypyrrole-coated colloidosomes are much less prone to collapse under UHV conditions compared to uncoated colloidosomes. This suggests that the polypyrrole overlayer reinforces the latex superstructure. Second, the polypyrrole overlayer has a relatively high Hamaker constant<sup>38</sup> and SEM images suggest that the polypyrrole-coated microcapsules are somewhat agglomerated. The higher magnification images in Figure 11 also suggest that the polypyrrole overlayer has filled in the latex interstices.

This hypothesis is supported by our dye release data for these microcapsules. Fluorescein dye is rapidly released from uncoated cross-linked colloidosomes: over 80% dye release occurred within just 5 h and 100% release was observed after 10 h (see Figure 9). Coating the same colloidosomes with 0.66 wt % polypyrrole (estimated conducting polymer thickness ~60 nm) reduced the rate of release such that only 50% of the dye was released in the first 5 h, with 96% release requiring 20 h. If the polypyrrole

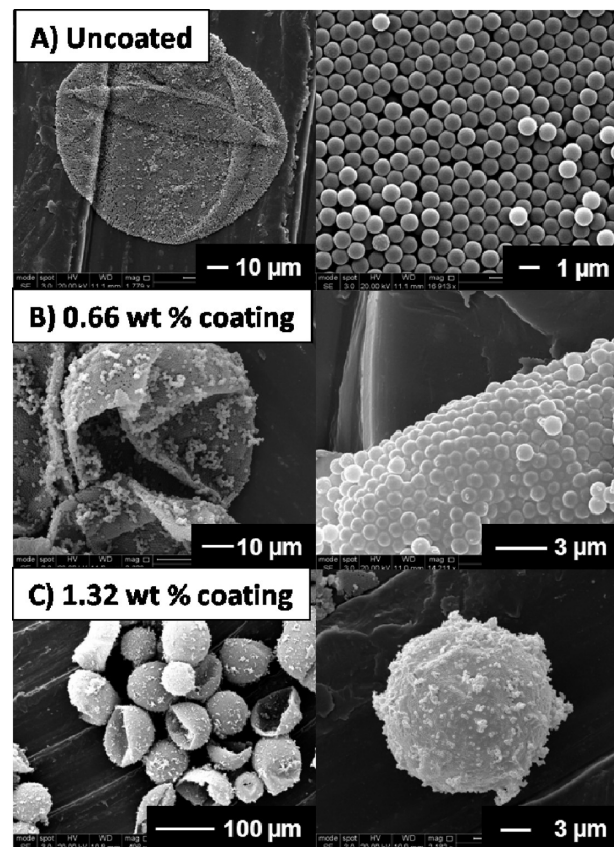


**Figure 11.** Scanning electron micrographs of cross-linked colloidosomes prepared with 1188 nm PGMA<sub>50</sub>–PS latex and sunflower oil encapsulated with fluorescein dye: (A) no polypyrrole, (B) 0.66 wt % polypyrrole loading, and (C) 1.32 wt % polypyrrole loading.

loading is doubled in thickness to 1.32 wt % (estimated conducting polymer thickness ~120 nm) the rate of dye release is retarded further: only 24% dye release occurred in the first 5 h, with 39% dye release obtained after 20 h. Thus, utilizing an additional polypyrrole overlayer allows the release of a small molecule dye from colloidosomes to be retarded significantly. The actual polypyrrole thickness could be up to half of that calculated since the hemispheres of the PS latex protruding from the oil surface can increase the droplet surface area by a factor of 2.<sup>39</sup>

In principle, reducing the dimensions of the interstices between adjacent latex particles within the colloidosome shell might be expected to lead to more effective annealing. However, when dye release studies were conducted on colloidosomes prepared with the smaller 107 nm latex (both with and without a polypyrrole coating of 30 nm), similarly disappointing dye retention results were obtained (data not shown). This may indicate that any advantage offered by smaller interstices may be offset by the higher permeability of a thinner latex shell. There is some recent literature precedent to support this hypothesis.<sup>40</sup>

Many commercial applications require encapsulated actives to have a shelf life of at least 12–18 months, which would require far more efficient encapsulation than these latex-based colloidosomes can currently offer. A capsule that originates from an organic/latex particulate shell has inherent problems regarding its porosity and encapsulation capability. Our attempts to close every individual interstitial hole have proven problematic, especially for the larger packing defects that inevitably originate from the intrinsic “scars” discussed earlier.<sup>30</sup> Even in cases where it appears that no latex interstices remain, such as in the work of Yow and Routh,<sup>33</sup> the long-colloidosomes term retention of small molecules within these remains a substantial technical challenge.



## Conclusions

In conclusion, we have developed a convenient route to covalently cross-linkable colloidosomes using hydroxy-functionalized sterically stabilized polystyrene latexes and a cheap, commercially available oil-soluble polymeric diisocyanate. The cross-linking is confined to the oil phase, with no evidence for any intercolloidosome fusion even at 50 vol %. In contrast, significant agglomeration can occur when cyclohexane-mediated annealing of the colloidosomes is attempted. The relative merits of utilizing two different sized latexes are readily apparent from our studies. The micrometer-sized latexes prepared by dispersion polymerization facilitate imaging of the resulting colloidosomes by SEM and fluorescence/optical microscopy. On the other hand, the smaller 107 nm latex prepared by emulsion polymerization allows monitoring of the cross-linking reaction by  $^1\text{H}$  NMR spectroscopy. Varying the latex concentration allows the mean oil droplet diameter to be tuned to some extent. Above a certain critical latex concentration, which corresponds to the limiting droplet diameter (and depends on the latex diameter), any additional latex simply remains in the aqueous phase. Below this critical concentration, larger oil droplets are obtained, but in each case we estimate an experimental latex packing efficiency of approximately 0.85. This relatively efficient packing is supported by high magnification images of the surface of individual colloidosomes, since hexagonal close-packing within the self-assembled latex monolayer is observed. Dye release studies have been conducted on these colloidosomes both with and without annealing of the latex particles and also with an additional conducting polymer coating. The cross-linked colloidosomes fail to retard dye release when compared to a control experiment involving just sunflower oil. More surprisingly, no improvement was observed when cyclohexane annealing was conducted in order to close the latex interstices. This suggests that either this annealing was incomplete or that the annealed shells are highly permeable. Coating the cross-linked colloidosomes in a thin layer of polypyrrole offers a significant improvement with respect to dye release, with thicker coatings leading to slower release. However, such latex-based microcapsules do not currently provide a practical means of encapsulating small molecules over relatively long time scales (e.g., months or years). Nevertheless, colloidosomes may yet offer potential biological applications where encapsulation of relatively large entities (cells, enzymes etc.) is desired in combination with high permeability of small molecules across the microcapsule wall. In this case the cross-linked stabilizer chains should act as a macromolecular “mesh” to aid retention of the encapsulated relatively large bioactive entities.

**Acknowledgment.** We thank the EPSRC for a Ph.D. studentship and P & G (Newcastle, UK) for CASE support for K.L.T. I. A. thanks the Higher Education Commission of Pakistan for funding a 6 month stay, under the International Research Support Initiative Programme (IRSIP), at the University of Sheffield. J.R. H. and S.E. acknowledge the EPSRC: Grant No. EP/G04077X/1.

**Supporting Information Available:** Figures showing  $^1\text{H}$  NMR and FT-IR spectra recorded for PPG-TDI cross-linked colloidosomes, SEM images of cyclohexane annealed colloidosomes both in the presence and absence of PPG-TDI, and visible absorption spectrum and absorbance vs concentration plot for fluorescein dye at pH 9. This material is available free of charge via the Internet at <http://pubs.acs.org>.

## References and Notes

- (1) Yow, H. N.; Routh, A. F. *Soft Matter* **2006**, *2*, 940–949.
- (2) Pickering, S. U. *J. Chem. Soc.* **1907**, *91*, 2001–2021.
- (3) Binks, B. P.; Lumsdon, S. O. *Phys. Chem. Chem. Phys.* **1999**, *1*, 3007–3016.
- (4) Levine, S.; Bowen, B. D.; Partridge, S. J. *Colloids Surf.* **1989**, *38*, 325–343.
- (5) Binks, B. P.; Lumsdon, S. O. *Langmuir* **2001**, *17*, 4540–4547.
- (6) Amalvy, J. I.; Armes, S. P.; Binks, B. P.; Rodrigues, J. A.; Unali, G. F. *Chem. Commun.* **2003**, *15*, 1826–1827.
- (7) Amalvy, J. I.; Unali, G. F.; Li, Y.; Granger-Bevan, S.; Armes, S. P.; Binks, B. P.; Rodrigues, J. A.; Whitby, C. P. *Langmuir* **2004**, *20*, 4345–4354.
- (8) Fujii, S.; Armes, S. P.; Binks, B. P.; Murakami, R. *Langmuir* **2006**, *22*, 6818–6825.
- (9) Fujii, S.; Randall, D. P.; Armes, S. P. *Langmuir* **2004**, *20*, 11329–11335.
- (10) Read, E. S.; Fujii, S.; Amalvy, J. I.; Randall, D. P.; Armes, S. P. *Langmuir* **2004**, *20*, 7422–7429.
- (11) Binks, B. P.; Murakami, R.; Armes, S. P.; Fujii, S. *Angew. Chem., Int. Ed.* **2005**, *44*, 4795–4798.
- (12) Ngai, T.; Auweter, H.; Behrens, S. H. *Macromolecules* **2006**, *39*, 8171–8177.
- (13) Velev, O. D.; Furusawa, K.; Nagayama, K. *Langmuir* **1996**, *12*, 2374–2384.
- (14) Velev, O. D.; Furusawa, K.; Nagayama, K. *Langmuir* **1996**, *12*, 2385–2391.
- (15) Velev, O. D.; Nagayama, K. *Langmuir* **1997**, *13*, 1856–1859.
- (16) Dinsmore, A. D.; Hsu, M. F.; Nikolaidis, M. G.; Marquez, M.; Bausch, A. R.; Weitz, D. A. *Science* **2002**, *298*, 1006–1009.
- (17) Laib, S.; Routh, A. F. *J. Colloid Interface Sci.* **2008**, *317*, 121–129.
- (18) Cayre, O. J.; Noble, P. F.; Paunov, V. N. *J. Mater. Chem.* **2004**, *14*, 3351–3355.
- (19) Noble, P. F.; Cayre, O. J.; Alargova, R. G.; Velev, O. D.; Paunov, V. N. *J. Am. Chem. Soc.* **2004**, *126*, 8092–8093.
- (20) Duan, H. W.; Wang, D. Y.; Sobal, N. S.; Giersig, M.; Kurth, D. G.; Mohwald, H. *Nano Lett.* **2005**, *5*, 949–952.
- (21) Croll, L. M.; Stöver, H. D. H. *Langmuir* **2003**, *19*, 5918–5922.
- (22) Skaff, H.; Lin, Y.; Tangirala, R.; Breitenkamp, K.; Böker, A.; Russell, T. P.; Emrick, T. *Adv. Mater.* **2005**, *17*, 2082.
- (23) Shah, R. K.; Kim, J. W.; Weitz, D. A. *Langmuir* **2010**, *26*, 1561–1565.
- (24) Thompson, K. L.; Armes, S. P. *Chem. Commun.* **2010**, *46*, 5274–6.
- (25) Thompson, K. L.; Armes, S. P.; York, D. W.; Burdis, J. A. *Macromolecules* **2010**, *43*, 2169–2177.
- (26) Lascelles, S. F.; Armes, S. P. *Adv. Mater.* **1995**, *7*, 864–868.
- (27) Balmer, J. A.; Armes, S. P.; Fowler, P. W.; Tarnai, T.; Gaspar, Z.; Murray, K. A.; Williams, N. S. J. *Langmuir* **2009**, *25*, 5339–5347.
- (28) Aveyard, R.; Binks, B. P.; Clint, J. H. *Adv. Colloid Interface Sci.* **2003**, *100–102*, 503–546.
- (29) Tambe, D. E.; Sharma, M. M. *Adv. Colloid Interface Sci.* **1994**, *52*, 1–63.
- (30) Bausch, A. R.; Bowick, M. J.; Cacciuto, A.; Dinsmore, A. D.; Hsu, M. F.; Nelson, D. R.; Nikolaidis, M. G.; Travesset, A.; Weitz, D. A. *Science* **2003**, *299*, 1716–1718.
- (31) It is worth emphasizing that neither methanol nor 2-propanol are suitable in this regard. The former is not miscible with *n*-alkanes, while the latter is a poor solvent for the PGMA stabilizer chains (and hence the latex).
- (32) Walsh, A.; Thompson, K. L.; Armes, S. P.; York, D. W. *Langmuir* **2010**, DOI: 10.1021/la103804y.
- (33) Yow, H. N.; Routh, A. F. *Langmuir* **2009**, *25*, 159–166.
- (34) *Polymer Handbook*, 2nd ed.; Wiley Interscience: New York, p IV-248.
- (35) Yuan, Q.; Cayre, O. J.; Fujii, S.; Armes, S. P.; Williams, R. A.; Biggs, S. *Langmuir* **2010**, DOI: 10.1021/la1033564.
- (36) Lavis, L. D.; Rutkoski, T. J.; Raines, R. T. *Anal. Chem.* **2007**, *79*, 6775–6782.
- (37) Armes, S. P. *Synth. Met.* **1987**, *20*, 365–371.
- (38) Markham, G.; Obey, T. M.; Vincent, B. *Colloids Surf.* **1990**, *51*, 239–253.
- (39) Maeda, S.; Armes, S. P. *Synth. Met.* **1995**, *73*, 151–155.
- (40) Rosenberg, R. T.; Dan, N. R. *J. Colloid Interface Sci.* **2010**, *349*, 498–504.